

## **Corrosion protection of transport vehicles by nanocoating of decahydrobenzo[8] annulene-5, 10-dihydrazone and SiC filler in H<sub>2</sub>O, O<sub>2</sub> (moist), CO<sub>2</sub>, SO<sub>2</sub> environments and weather change**

**RAJESH KUMAR SINGH**

Department of Chemistry, Jagdam College, JP University, Chapra-841301, India

**Abstract :** Transport industries use epoxy-coating for corrosion protection of stainless steel but this coating cannot provide protection in long duration in H<sub>2</sub>O, O<sub>2</sub> (moist), CO<sub>2</sub> and SO<sub>2</sub> environment and weather change. Pollutants can create acidic medium for epoxy-coated stainless steel. These corrosive agents penetrate epoxy-coating by osmosis or diffusion process produce and produce chemical and corrosion reactions with base metal. These reactions enhance internal and external corrosion and accelerate internal disbonding in epoxy-coating and disintegrate base metal. This coating does not protect themselves and base metal. These pollutants and weather change elevate galvanic, pitting, stress, crevice, intergranular, blistering and embrittlement corrosion whereas epoxy polymer exhibits swelling and dissolving corrosion. Pollutants and weather change can alter their physical, chemical and mechanical properties and tarnish their facial appearance. They can also change morphology epoxy-coated stainless steel.

Corrosion mitigation of epoxy-coated stainless steel in ambient of H<sub>2</sub>O, O<sub>2</sub> (moist), CO<sub>2</sub> and SO<sub>2</sub> and weather change used nanocoating and filler technology. For this work decahydrobenzo<sup>[8]</sup> annulene-5, 10-dihydrazone and SiC used as nanocoating and filler materials. Nanocoating and filling work were completed by nozzle spray. The corrosion rate of epoxy-coated stainless steel coupons was determined at 278, 283, 288, 293 and 2980K temperatures and times mentioned at these temperatures was 24, 48, 72, 96 and 120 hours in different weather without coating and with nanocoating of decahydrobenzo<sup>[8]</sup> annulene-5, 10-dihydrazone and SiC filler by help of weight loss experiment. Corrosion potential and corrosion current were determined by potentiostat. Coating efficiency and surface coverage area were calculated by gravimetric methods. The surface composite barrier formation was studied by activation energy, heat of adsorption, free energy, entropy and enthalpy.

**Keywords :** Corrosion protection, Transport industries, Epoxy coatings, SO<sub>2</sub> environment, Weather / environmental changes and corrosion.

### **INTRODUCTION**

Corrosion is major problem with materials due to atmospheric pollutants. It cannot fully control but it is minimized by application certain protection techniques. Metallic coating used for corrosion protection in acidic medium<sup>[1]</sup>. It did not produce good result in this environment. Paint coating is better option to protect materials from atmospheric pollutants. This coating is not give good results because the coating materials<sup>[2]</sup> form a permeable barrier on the surface of base by the process of osmosis or diffusion corrosive gases enter inside and absorb moisture to produce acids which corrodes metal and initiate disbonding between coating substance<sup>[3]</sup>. Polymeric materials are laminated on the surface of metal to protect from the attack of corrosive gases. These laminations<sup>[4]</sup> do not provide satisfactory results in such environment.

\*Corresponding Authors Email : rks\_jpujc@yahoo.co.in

Polymeric laminated metal outer surface has lot of porosities which accelerate osmosis reaction thus deterioration starts between them. Highly electron rich organic compounds contain nitrogen, oxygen and sulphur are used as inhibitors to check corrosion of materials in acidic environment. These inhibitors form a thin surface film on metal surface that protective barrier<sup>[5]</sup> do not protect metal in such corrosive ambient. The ability of a coating to protect a given metal against corrosion generally depends on the quality of the coating, the metal characteristics and the properties of the metal/coating interface. No coating is impenetrable and therefore ions, oxygen and water will diffuse towards the metal surface with a rate and to an extent determine<sup>[6]</sup> by the coating used and the environment.

The transport<sup>[7]</sup> through a coating on a metal surface is an example of mixed transport, i.e. tow transport processes, the transport of charge and mass take place at the same time. The ability of a coating to be semi permeable and of some coatings to ion exchangers complicates the question of transport through coatings further.

The permeability of ions, water and oxygen through free films<sup>[8]</sup> has been studied for a number of different coatings. The permeability of water vapour has been found to be about  $1\text{mg}/\text{cm}^2/\text{day}$  of the corrosion reaction on coated steel surfaces. The transport of oxygen gas, however, may according to the measurements done, be the rate determining factor in some cases. The transport through a coating will, however, depend on the reactions at the steel surface. For given environment and transport properties of the coatings, the initiation of corrosion and the type of corrosion attack on coated metal surfaces<sup>[9]</sup> depend on the properties of the metal the metal/coating interface.

On coated steel surface<sup>[10]</sup> the corrosion attacks are initiated at weak points of the coating or in mechanically damaged areas. The remaining surface generally acts as a cathode. This may increase the rate of corrosion in the damaged area depending on the cathodic properties of the coated surface, the coating resistance. The coating in the cathodic area may be disbanded.

Cathodic disbanding<sup>[11]</sup>, i.e. loss of adhesion due to the cathodic reaction is a common mode of failure of coated steel surfaces. The detailed mechanisms are unknown, but in an air saturated electrolyte disbanding is usually caused by the oxygen reaction and it is the high pH generated by this reaction that is considered to be most important.

The aim of this investigation has been to study the cathodic reaction on coated steel surfaces and to see if there is any connection between the rate of this reaction and the ability of a coating to protect against corrosion.

Although the combined application of plastic coating<sup>[12]</sup> and cathodic protection has become a widespread and general technology for preventing corrosion on buried steel pipelines, corrosion failures are still occasionally experienced, among others under disbanded coatings.

The significance of coating disbonding has increasingly been realized since the first recognition of disbondings as a possible origin of environmentally assisted failures such as the carbonate-bicarbonate stress corrosion cracking and the hydrogen stress cracking<sup>[13]</sup> of high pressure pipelines.

Recent field and laboratory studies have shown that these failures are all closely related to the conditions of cathodic protection<sup>[14]</sup> within the crevice formed between a disbonded coating<sup>[15]</sup> and a piece of pipe steel. It I believed that the very thin crevice under the disbanded coating allows relatively limited amount of water, chemical species and cathodic current to pass

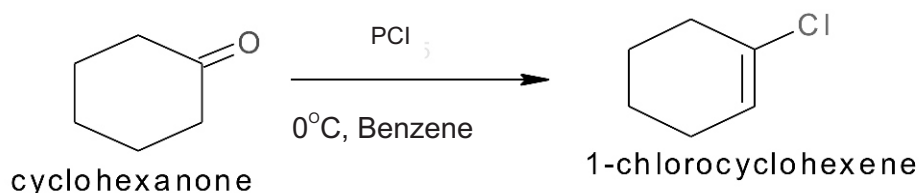
through it, preventing the escape of alkaline water and reducing the full effect of the cathodic protection<sup>[16]</sup>, and thereby developing a more favorable condition for the stress corrosion cracking. Nanocoating of decahydrobenzo<sup>[8]</sup> annulene-5, 10-dihyrazone and SiC filler formed a composite thin film barrier on the surface of epoxy-coated stainless steel.

## EXPERIMENTAL

The epoxy-coated stainless steel coupon was kept in H<sub>2</sub>O, O<sub>2</sub> (moist), CO<sub>2</sub> and SO<sub>2</sub> environment and the corrosion rate sample was calculated required without coating and with coating at mentioned 278, 283, 288, 293 and 2980K temperatures and times 24, 48, 72, 96 and 120 hours as weather change. These results were recorded by gravimetric methods. Coating work was completed by nozzle spray. Acidic natures of gases were determined by application of pH meter. The composite surface film formation results were determined by activation energy, heat of adsorption, free energy, enthalpy and entropy. Potentiostat 158 EG & G Princeton Applied for recording corrosion potential and corrosion current density of decahydrobenzo<sup>[8]</sup> annulene-5, 10-dihyrazone and SiC. The nanocoating product was synthesized by given below methods.

### Synthesis of decahydrobenzo<sup>[8]</sup> annulene-5, 10-dihyrazone

Cyclohexanone (80g) was added in dry benzene (150ml) and reaction mixture was poured drop wise into a cool solution of PCI<sub>5</sub>. The mixture was taken in two necks round bottle flask and stirred for further 3hours and during reaction temperature was maintained 0°C. The product was extracted from ethereal solution and was washed with 5% aqueous Na<sub>2</sub>CO<sub>3</sub> then after dried with Na<sub>2</sub>SO<sub>4</sub> and solvent removed by application of rotator vapour. The product was purified by column chromatograph by the use of silica gel in petroleum ether. After purification 87% of 1-chlorocyclohexene was obtained.

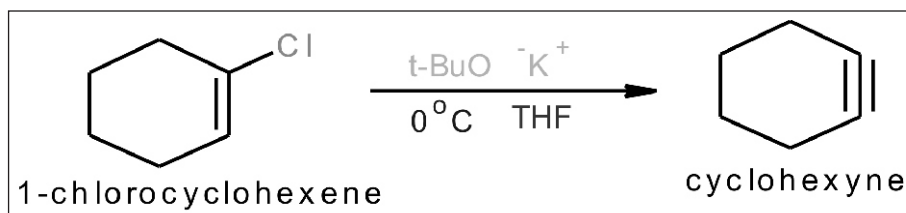


### Physical properties of 1-chlorocyclohexene

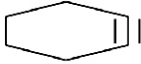
#### <sup>1</sup>H NMR of 1-chlorocyclohexene

	Molecular Formula	= C <sub>6</sub> H <sub>9</sub> Cl
	Formula Weight	= 116.58866
	Composition	= C (61.81%) H (7.78%) Cl (30.41%)
	Molar Refractivity	= 32.29 ± 0.4 cm <sup>3</sup>
	Molar Volume	= 113.5 ± 5.0 cm <sup>3</sup>
	Parachor	= 263.4 ± 6.0 cm <sup>3</sup>
	Index of Refraction	= 1.480 ± 0.03
	Surface Tension	= 29.0 ± 5.0 dyne/cm
	Density	= 1.02 ± 0.1 g/cm <sup>3</sup>
	Dielectric Constant	= Not available
	Polarizability	= 12.80 ± 0.5 10 <sup>-24</sup> cm <sup>3</sup>
	Monoisotopic Mass	= 116.039278 Da
	Nominal Mass	= 116 Da
	Average Mass	= 116.5887 Da
	M <sup>+</sup>	= 116.038729 Da
	M <sup>-</sup>	= 116.039827 Da
[M + H] <sup>+</sup>	= 117.046554 Da	
[M + H] <sup>-</sup>	= 117.047652 Da	
[M - H] <sup>+</sup>	= 115.030904 Da	
[M - H] <sup>-</sup>	= 115.032002 Da	

1-Chlorocyclohexene (57g) was dissolved in THF and potassium t-butoxide (BuOK<sup>+</sup>) was added (75g) at room temperature then after cyclohexene (70ml) was mixed into reaction mixture as trapping agent. After completion of reaction water was poured then it quenched with brine solution and reaction mixture was extracted from ether. Finally, the compound was dried with sodium sulphate. Solvent was removed by rotator vapour and target product was purified by silica gel column chromatograph. After purification 83% yield of 1, 2, 3, 4, 4a, 5, 6, 7, 8, 8b-decahydrobipthalene was obtained.



### Physical properties of cyclohexyne

	Molecular Formula	= C <sub>6</sub> H <sub>8</sub>
	Formula Weight	= 80.12772
	Composition	= C (89.94%) H (10.06%)
	Molar Refractivity	= 25.79 ± 0.4 cm <sup>3</sup>
	Molar Volume	= 91.7 ± 5.0 cm <sup>3</sup>
	Parachor	= 217.9 ± 6.0 cm <sup>3</sup>
	Index of Refraction	= 1.474 ± 0.03
	Surface Tension	= 31.8 ± 5.0 dyne/cm
	Density	= 0.87 ± 0.1 g/cm <sup>3</sup>
	Dielectric Constant	= Not available
	Polarizability	= 10.22 ± 0.5 10 <sup>-24</sup> cm <sup>3</sup>
	Monoisotopic Mass	= 80.0626 Da
	Nominal Mass	= 80 Da
	Average Mass	= 80.1277 Da
	M <sup>+</sup>	= 80.062052 Da
	M <sup>-</sup>	= 80.063149 Da
	[M + H] <sup>+</sup>	= 81.069877 Da
	[M + H] <sup>-</sup>	= 81.070974 Da
	[M - H] <sup>+</sup>	= 79.054227 Da
	[M - H] <sup>-</sup>	= 79.055324 Da

### H1NMR of cyclohexyne

**ChemNMR <sup>1</sup>H Estimation** of cyclohexyne

Estimation quality is indicated by color: good, medium, rough

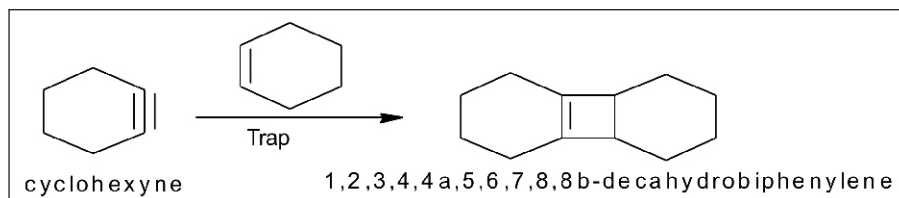
Protocol of the H-1 NMR Prediction (Lib=SU Solvent=DMSO 300 MHz):

Node	Shift	Base + Inc.	Comment (ppm rel. to TMS)
CH2 1.96	1.37	0.65	methylene
		-0.06	1 alpha -C+C-C
		-0.06	1 beta -C
CH2 1.96	1.37	0.65	methylene
		-0.06	1 alpha -C+C-C
		-0.06	1 beta -C
CH2 1.44	1.37	0.13	methylene
		-0.06	1 beta -C+C-C
		-0.06	1 beta -C
CH2 1.44	1.37	0.13	methylene
		-0.06	1 beta -C+C-C
		-0.06	1 beta -C

**<sup>1</sup>H NMR Coupling Constant Prediction**

shift	atom index	coupling partner	constant and vector
1.96	3	5	7.1 H-CH-CH-H
		4	2.5 H-CH-C+C-CH-H
1.96	4	6	7.1 H-CH-CH-H
		3	2.5 H-CH-C+C-CH-H
1.44	5	3	7.1 H-CH-CH-H
		6	7.1 H-CH-CH-H
1.44	6	4	7.1 H-CH-CH-H
		5	7.1 H-CH-CH-H

Cyclohexene solution poured into cyclohexyne and reaction mixture was stirred one hours then cyclohexene trapped with cyclohexyne to form an adduct of decahydrobiphenylene.

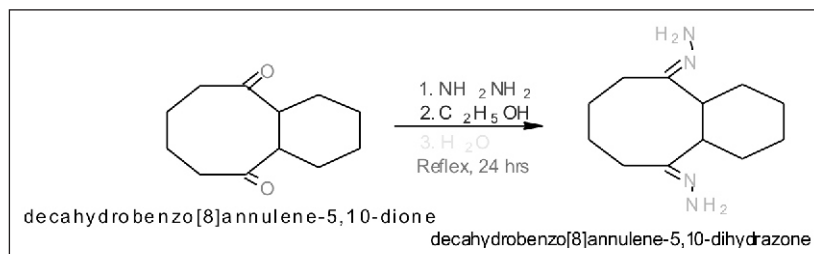


#### Physical properties of 1,2,3,4,4a,5,6,7,8,8b-decahydrobiphenylene

	Molecular Formula	= C <sub>12</sub> H <sub>18</sub>
	Formula Weight	= 162.27132
	Composition	= C(88.82%) H(11.18%)
	Molar Refractivity	= 50.88 ± 0.4 cm <sup>3</sup>
	Molar Volume	= 164.7 ± 5.0 cm <sup>3</sup>
	Parachor	= 398.2 ± 6.0 cm <sup>3</sup>
	Index of Refraction	= 1.529 ± 0.03
	Surface Tension	= 34.1 ± 5.0 dyne/cm
	Density	= 0.98 ± 0.1 g/cm <sup>3</sup>
	Dielectric Constant	= 2.79 ± 0.2
	Polarizability	= 20.17 ± 0.5 10 <sup>-24</sup> cm <sup>3</sup>
	Monoisotopic Mass	= 162.140851 Da
	Nominal Mass	= 162 Da
Average Mass	= 162.2713 Da	
M+	= 162.140302 Da	
M-	= 162.141399 Da	
[M+H] <sup>+</sup>	= 163.148127 Da	
[M+H] <sup>-</sup>	= 163.149224 Da	
[M-H] <sup>+</sup>	= 161.132477 Da	
[M-H] <sup>-</sup>	= 161.133574 Da	

#### H1NMR of 1,2,3,4,4a,5,6,7,8,8b-decahydrobiphenylene

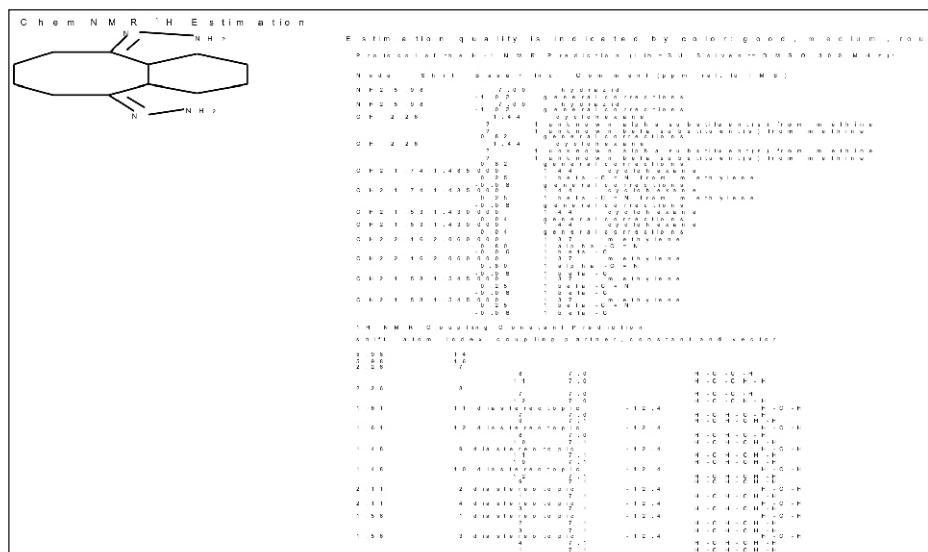
Decahydrobenzo<sup>[8]</sup> annulene-5, 10-dione (68g) was taken in a round bottomed flask and 85g of hydrazine hydrate was added and the mixture was heated under reflux for 24 hours. The solution was cooled in an ice bath and the decahydrobenzo<sup>[8]</sup> annulene-5, 10-dihydrazone was separated by suction filtration. The crystals were washed with 150 ml of cold ethanol and dried on the suction filter for 1 hour. The yield of decahydrobenzo<sup>[8]</sup> annulene-5, 10-dihydrazone 85% was obtained.



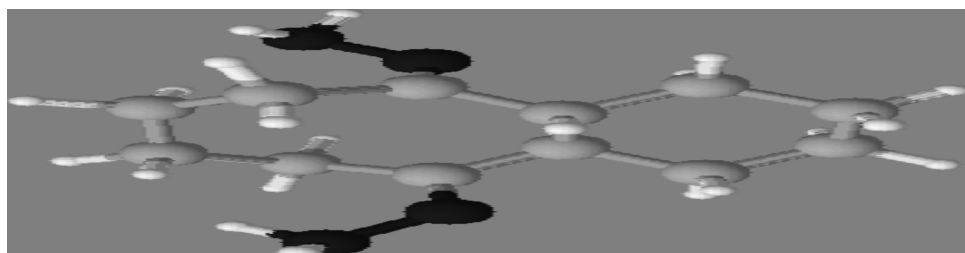
**Physical properties of decahydrobenzo<sup>[8]</sup>annulene-5,10-dihydrazone**

Molecular Formula	= C <sub>12</sub> H <sub>16</sub> N <sub>2</sub>
Formula Weight	= 222.32988
Composition	= C (64.83%) H (9.57%) N (25.20%)
Molar Refractivity	= 62.68 ± 0.5 cm <sup>3</sup>
Molar Volume	= 171.7 ± 7.0 cm <sup>3</sup>
Parachor	= 461.9 ± 8.0 cm <sup>3</sup>
Index of Refraction	= 1.650 ± 0.05
Surface Tension	= 52.3 ± 7.0 dyne/cm
Density	= 1.29 ± 0.1 g/cm <sup>3</sup>
Dielectric Constant	= Not available
Polarizability	= 24.85 ± 0.5 10 <sup>-24</sup> cm <sup>3</sup>
Monoisotopic Mass	= 222.18447 Da
Nominal Mass	= 222 Da
Average Mass	= 222.3299 Da
M+	= 222.183898 Da
M-	= 222.184995 Da
[M+H] <sup>+</sup>	= 223.191723 Da
[M+H] <sup>-</sup>	= 223.19262 Da
[M-H] <sup>+</sup>	= 221.176073 Da
[M-H] <sup>-</sup>	= 221.17717 Da

**H1NMR of decahydrobenzo<sup>[8]</sup>annulene-5,10-dihydrazone**



**XRD of decahydrobenzo<sup>[8]</sup>annulene-5,10-dihydrazone**



## RESULTS AND DISCUSSION

The corrosion rates of epoxy-coated stainless steel, nanocoated of decahydrobenzo<sup>[8]</sup> annulene-5, 10-diylienedihydrazine and SiC filler were calculated by equation  $K=13.56 X (W/A D t)$  and their results were written in table 1. It was observed in absence of coating the corrosion rate of epoxy-coated stainless steel increased but these values were reduced in presence of nanocoating and filler compounds. The results of table 1 indicate that without coating corrosion rate of epoxy-coated stainless enhance at lower temperature to higher temperature but these values minimize with nanocoating and filler compounds. Fig. 1 plotted between corrosion rate  $K(\text{mmpy})$  versus  $t(\text{hrs})$  indicated that corrosion rate increased with exposer times duration were long but nanocoating and filler compounds reduced corrosion rate as shown in figure. The corrosion rate of material is function of time, if materials expose in atmosphere in a longer duration without any protective substance, their corrosion rate accelerate. It is very difficult to control corrosion of epoxy-coated stainless steel corrosion but this technique give good results in above corrosive medium and weather change.

Table 1 Corrosion rate of epoxy-coated stainless steel with nanocoating of decahydrobenzo<sup>[8]</sup> annulene-5, 10-dihydrzone and SiC filler in  $\text{H}_2\text{O}$ ,  $\text{O}_2$  (moist),  $\text{CO}_2$  and  $\text{SO}_2$  environment and weather change

NC	Temp( <sup>0</sup> K)	278 <sup>0</sup> K	283 <sup>0</sup> K	288 <sup>0</sup> K	293 <sup>0</sup> K	298 <sup>0</sup> K	C(mM)
	Times (hrs.)	24	48	72	96	120	
NC(0)	$K_o$ log $K_o$	425 2.628	628 2.797	738 2.868	977 2.989	1021 3.001	0.0 50
NC(2)	K logK log(K/T) $\theta$ log( $\theta/1-\theta$ ) %CE	191 2.281 1.725 0.55 0.087 55	95 1.977 1.429 0.84 0.720 84	63 1.707 1.259 0.91 1.029 91	48 1.579 1.148 0.95 1.270 95	36 1.556 1.031 0.96 1.436 96	
NC(f)	K logK log(K/T) $\theta$ log( $\theta/1-\theta$ ) %CE	154 2.187 1.632 0.63 0.231 63	77 1.886 1.338 0.87 0.854 87	51 1.681 1.167 0.93 1.128 93	38 1.556 1.047 0.96 1.392 96	31 1.491 0.966 0.97 1.503 97	20

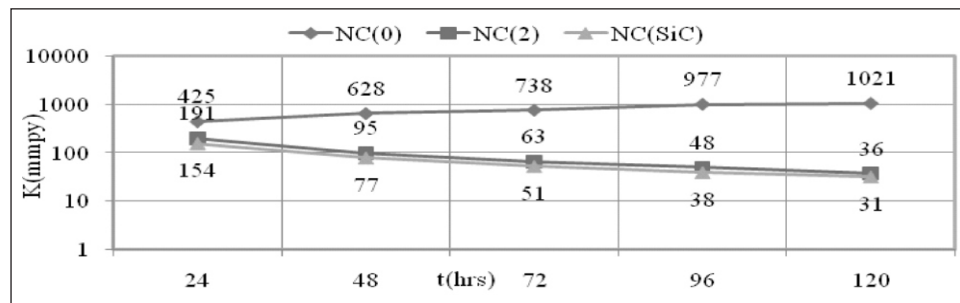


Fig. 1 : Plot of  $K$  Vs  $t$  epoxy-coated stainless steel with nanocoating of NC(2) and SiC filler



Corrosion rates of epoxy coated stainless steel, nanocoated decahydrobenzo<sup>[8]</sup> annulene-5, 10-dihydrazone and SiC filler were calculated at different temperatures and their values are mentioned in Table 4.3.1. Fig. 4.3.2 plotted between logK versus 1/T which indicated a straight line that the corrosion rate of epoxy-coated stainless steel reduced with nanocoating and filler material from lower to higher temperatures but its values enhance without coating. Decahydrobenzo<sup>[8]</sup> annulene-5, 10-dihydrazone is an electron rich compound which adheres to the surface of epoxy-coated stainless steel and SiC filler blocks porosities of nanocoating material. Fig. 4.3.2 shows that nanocoating and filler compounds reduced corrosion rate from lower to higher temperatures.

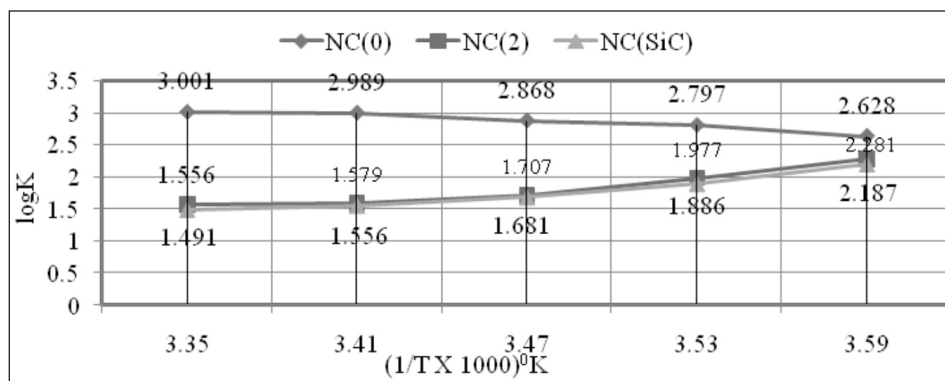


Fig. 2 : Plot of logKVs 1/T for epoxy-coated stainless steel with nanocoating of NC(2) & SiC filler

The values of log( $\theta/1-\theta$ ) for decahydrobenzo<sup>[8]</sup> annulene-5, 10-dihydrazone and SiC filler at 273 to 2980K were mentioned in Table 1. The results of Table 1 noticed that nanocoating and filler compounds enhanced the values of log( $\theta/1-\theta$ ) at lower to higher temperature. Fig. 3 drew between log( $\theta/1-\theta$ ) versus 1/T found to be a straight line which indicated that both compounds were increased their values as temperatures rise. The values of log( $\theta/1-\theta$ ) of both compounds were shown that they mitigated corrosion rate and enhanced stability of surface barrier.

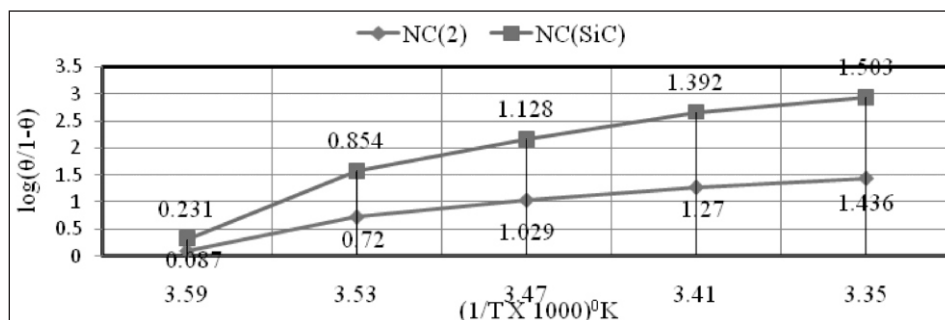


Fig 3 : Plot of log( $\theta/1-\theta$ ) Vs 1/T for epoxy-coated stainless steel with nanocoating of NC(2) & filler SiC

The surface coverage area ( $\theta$ ) was covered by decahydrobenzo<sup>[8]</sup> annulene-5, 10-dihydrazone and SiC filler at different temperatures were calculated by equation  $\theta = (1-K/K_0)$  and its values are written in Table 1. The surface coverage area increased with rising temperatures such effect is clearly reflected in figure 4 plotted between  $\theta$  (surface coverage area) versus T (temperature). In case of SiC filler enlarged the coating boundary of nanocoating compound and their coating barrier stability. The filler compound dispersed into matrix of nanocoated material and



developed a passive barrier which suppressed attack of H<sub>2</sub>O, O<sub>2</sub> (moist), CO<sub>2</sub> and SO<sub>2</sub>. Both nanocoating and filler compounds were formed a stable barrier that barrier did not decomposed at higher temperature.

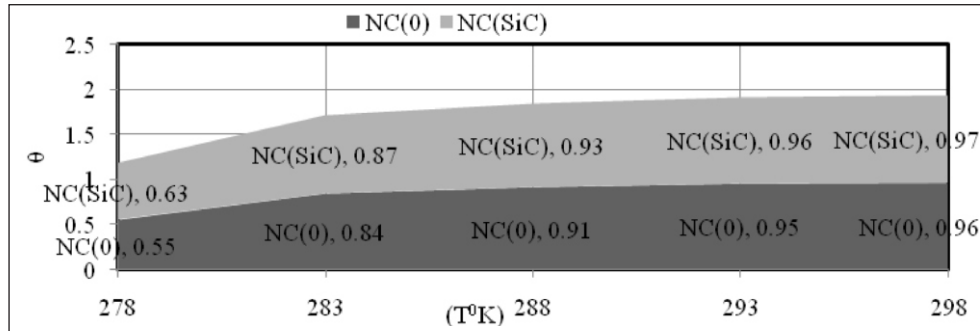


Fig. 4 : Plot of  $\theta$  Vs T epoxy-coated stainless steel with nanocoating NC(2) & SiC filler

Percentage coating efficiency of decahydrobenzo<sup>[8]</sup> annulene-5, 10-dihydrazone and SiC filler were determined by equation  $\%CE = (1-K/K_0) \times 100$  and their values are written in Table 1. The plot between percentages coating efficiency (%CE) versus temperature (T) is represented in Fig. 5 which indicates that coating efficiency of nanocoating compound was increased by SiC filler. The filler compound entered into porosities of nanocoating compound and produced nonpermeable thin film layer on the surface of base material. This barrier layer can stop osmosis or diffusion process of corrosion pollutants.

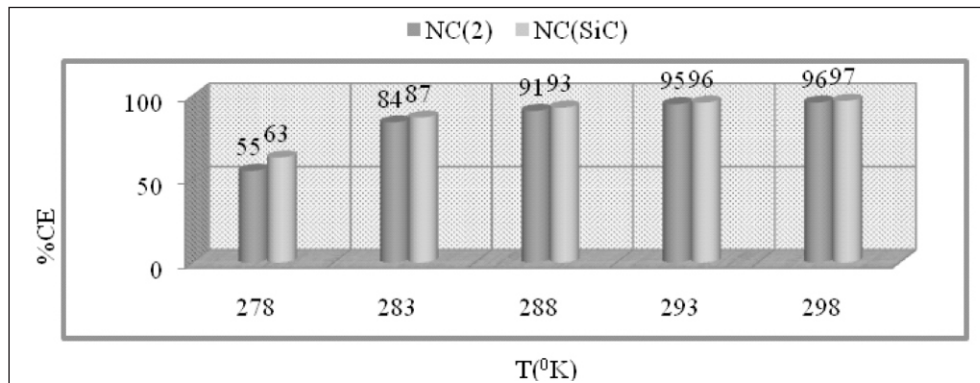


Fig. 5 : Plot of %CE Vs T for epoxy-coated stainless steel with nanocoating of NC(2) & SiC filler

Nanocoating compound decahydrobenzo<sup>[8]</sup> annulene-5, 10-dihydrazone and SiC filler surface thin film formation, bond formation, adsorption properties, types of reaction, stability and permeability barrier were studied by activation energy, heat of adsorption, free energy, enthalpy and entropy.

Activation energy of decahydrobenzo<sup>[8]</sup> annulene-5, 10-dihydrazone and SiC filler were calculated by Arrhenius equation  $d/dT(\ln K) = A_e - E_a/RT$  and Fig. 2 plotted between  $\log K$  versus  $1/T$  and their values are mentioned in Table 2. The results of Table 2 show that without coating activation energy values were high but after coating its values decreased as temperature enhanced. These results indicate that nanocoating and filler compounds formed chemical bonding with base material.

Heat of adsorption for nanocoating and filler compounds were determined by equation  $\log(\theta/1-\theta) = \log(AC) - (q/2.303RT)$  and Fig. 3 and their values were expressed in Table 2. Heat of adsorption values found to be negative in both compounds. It confirmed that nanocoating and filler compounds attached with epoxy-coated stainless steel by chemical bonding.

The negative sign of free energy indicated that nanocoating of decahydrobenzo<sup>[8]</sup> annulene-5, 10-dihydrazone and SiC filler developed chemical bonding during coating and this process is exothermic and their values were obtained by equation  $-\Delta G = -2.303 \log(33.3K)$ . The values of nanocoating and filler compounds are recorded in Table 2. Both compounds free energy values were shown that nanocoating and filler materials formed thin surface barrier. SiC free energies were at different temperatures indicated that they formed chemical bonding with decahydrobenzo<sup>[8]</sup> annulene-5, 10-dihydrazone.

Enthalpy and entropy of nanocoating and filler materials were calculated by transition state equation  $K = R T / N h \log(\theta S\# / R) X \log(-\theta H\# / R T)$  and figure6 and their values are recorded in table2. Enthalpy and entropy values were found to be negative with both compounds and their values confirmed that coating and filling processes were an exothermic reaction. The coating barriers developed by these compounds were highly ordered and they were adhered with epoxy-coated stainless steel by chemical bonding. Decahydrobenzo[8]annulene-5,10-dihydrazone and SiC entropies indicated that these compounds were located on the surface of base metal by order ways. Decahydrobenzo[8]annulene-5,10-dihydrazone and SiC create a passive barrier that is stable in high temperature and corrosive medium.

Table 2 Thermal parameters values of decahydrobenzo<sup>[8]</sup> annulene-5, 10-dihydrazone and SiC filler for epoxy-coated stainless steel at different temperatures

Thermal parameters	278 <sup>0</sup> K	283 <sup>0</sup> K	288 <sup>0</sup> K	293 <sup>0</sup> K	298 <sup>0</sup> K
NC(0)Ea	180	191	192	197	195
NC(2) Ea	149	126	112	102	91
NC(2)q	-18.40	-58.41	-74.34	-90.02	-96.70
NC(2)ΔG	-254	-229	-213	-201	-189
NC(2)ΔH	-110	-89	-76	-67	-58
NC(2)ΔS	-101	-90	-83	-78	-74
θ NC(2)	0.55	0.84	0.91	0.95	0.96
NC(SiC)Ea	140	119	105	93	88
NC(SiC)q	-28.10	-67.79	-84.83	-98.43	-108.01
NC(SiC)ΔG	-247	-222	-206	-195	-186
NC(SiC)ΔH	-104	-82	-69	-61	-54
NC(SiC)ΔS	-98	-86	-79	-75	-71
θNC(SiC)	0.63	0.87	0.93	0.96	0.97

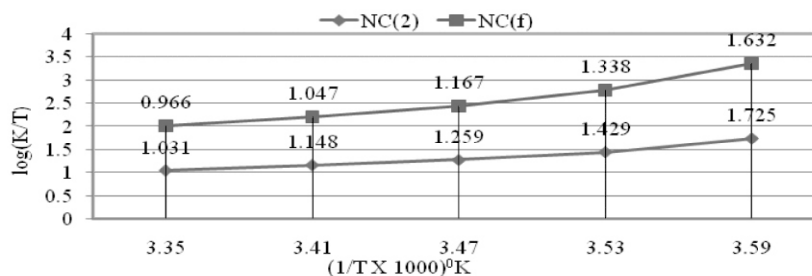


Fig. 6 : log(K/T) Vs 1/T for epoxy-coated stainless steel with nanocoating of NC(2) & SiC filler

Fig. 7 plotted among enthalpy ( $\Delta H$ ), entropy ( $\Delta S$ ), surface coverage area ( $\theta$ ) versus temperature ( $T^{\circ}K$ ). This figure indicates enthalpy and entropy were decreased when temperature of nanocoating and filler compounds increased. It also shows that surface coverage area was enhanced when enthalpy and entropy vales of nanocoating and filler compounds reduced.

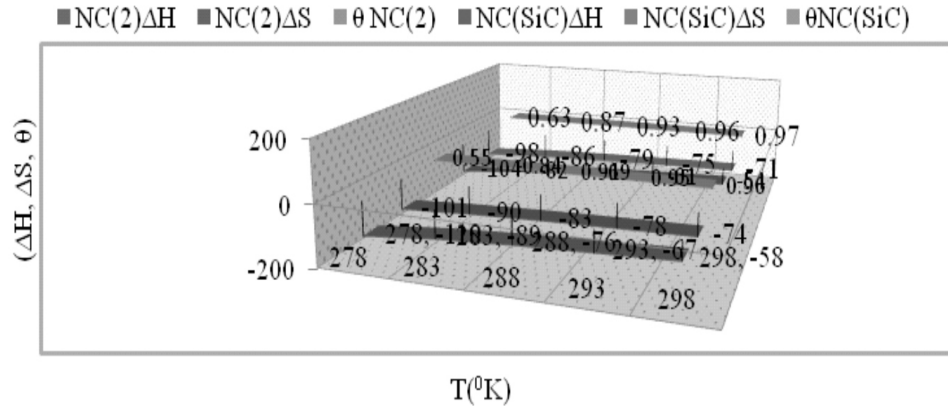


Fig. 7 : Plot of  $\Delta H$ ,  $\Delta S$ ,  $\theta$  Vs  $T^{\circ}K$  forepoxy-coated stainless steel nanocoating of NC(2) & filler SiC

Potentiostat polarization results of nanocoating decahydrobenzo<sup>[8]</sup> annulene-5, 10-dihydrazone and SiC filler were calculated by equation  $\Delta E/\Delta I = \beta_a \beta_c / 2.303 I_{corr} (\beta_a + \beta_c)$  and figure 8 and their values are written in Table 3. The plot between electrode potential ( $\Delta E$ ) versus corrosion current density ( $I_{corr}$ ) are mentioned in Fig. 8 that plot confirmed cathodic polarization increasing whereas anodic polarization decreasing.

Corrosion current of epoxy-coated stainless steel, decahydrobenzo<sup>[8]</sup> annulene-5, 10-dihydrazone and SiC filler were determined by above equation and their values put in equation,  $C.R. (mmpy) = 0.1288 I_{corr} (mA/cm^2) \times Eq.Wt (g) / \rho (g/cm^3)$  to produce corrosion rate of all three material. The results of Table 3 expressed that nanocoating and filler compounds decreased corrosion rate and increased surface coverage area and coating efficiency. Potentiostatic results of SiC observed that it enhanced corrosion current density and surface coverage area in hostile environment. The results of epoxy-coated stainless steel, decahydrobenzo<sup>[8]</sup> annulene-5, 10-dihydrazone and SiC obtained by weight loss method satisfied the results of potentiostat.

Table 3 Potentiostat results of epoxy-coated stainless steel of decahydrobenzo<sup>[8]</sup> annulene-5, 10-dihydrazone and SiC filler compounds in  $H_2O$ ,  $O_2$  (moist),  $CO_2$  and  $SO_2$  environment.

NC	$\theta E$ (mV)	$\theta I$	$\beta_a$	$\beta_c$	$I_{corr}$ (mA/cm <sup>2</sup> )	K (mmpy)	$\theta$	%CE	C(mM)
NC(0)	-704	187	295	197	13.64	417	0	0	0.0
NC(2)	-301	36	62	275	2.63	81	0.81	71	50
NC(SiC)	-281	30	52	287	2.04	62	0.85	85	20

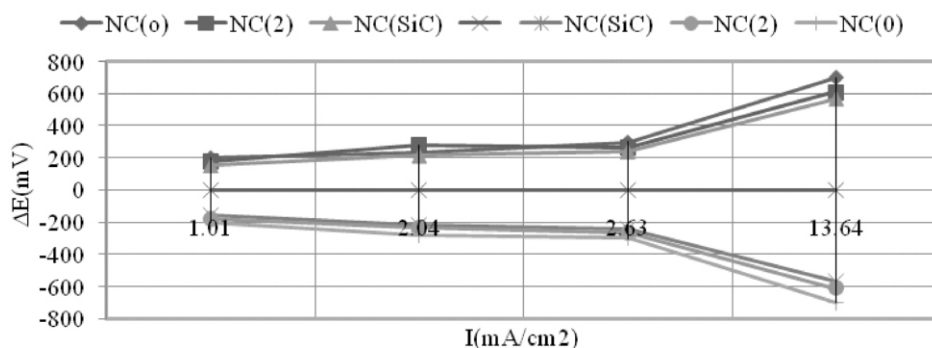


Fig. 8 : Plot of  $\Delta E$  Vs  $I$  epoxy-coated stainless steel with nanocoating of NC(2) & filler SiC

## CONCLUSION

The results of weight loss experiments, potentiostat and thermal parameters were shown that nanocoating compound decahydrobenzo<sup>[8]</sup> annulene-5, 10-dihydrazone and SiC filler were formed a composite-thin-film-barrier on the surface of base materials. It shows that coating barrier is stable at different temperatures and weathers. The nanocoating and filler compounds were adhered with base materials by chemical bonding. The composite-thin-film-barrier works as repeller for corrosive pollutants. The filler compound blocks porosities which are developed by nanocoating material and increases internal binding force among.

## ACKNOWLEDGEMENT

Author thanks to the UGC-New Delhi providing financial support for this work. Author gives regards the HOD, Department of Applied chemistry ISM, Dhanbad who provides laboratory facilities.

## REFERENCES

- [1] Bhadra S., Singh N.K. and Khastgir D., (2011), Polyaniline based anticorrosive and anti-molding coating, Journal of Chemical Engineering and Materials Science, **2**(1), pp. 1-11.  
Bibber J.W., (2009), Chromium free conversion coating for zinc and its alloys, Journal of Applied Surface Finishing, **2**(4), pp. 273-275.
- [2] Szabo T., Molnar-Nagy L. and Telegdi J., (2011), Self-healing microcapsules and slow release microspheres in paints, Progress in Organic Coatings, **72**, pp. 52-57.  
Videla H. and Herrera L.K., (2009), Understanding microbial inhibition of corrosion, Electrochem Acta, **39**, pp. 229-234.
- [3] Wen N.T., Lin C.S., Bai C.Y. and Ger M.D., (2008), Structures and characteristics of Cr (III) based conversion coatings on electrogalvanized steels, Surf. Coat. Technol, **203**, pp. 317.  
Boerio F.J., Shah P., (2005), Adhesion of injection molded PVC to steel substrates, J of Adhesion, **81**(6) pp. 645-675.
- [4] Deveci H., Ahmetti G. and Ersoz M., (2012), Modified styrenes: Corrosion physico-mechanical and thermal properties evaluation, Prog. Org. Coat., **73**. pp. 1-7.
- [5] Genzer J., (2005), Templating Surfaces with Gradient Assemblies, J of Adhesion, **81**, pp. 417-435.
- [6] Leon-Silva U. and Nicho M.E., (2010), Poly(3-octylthiophene) and polystyrene blends thermally treated as coating for corrosion protection of stainless steel 304, J. Solid State Electrochem, **14** **1**, pp. 487-1497.
- [7] Baier R.E., (2006), Surface behaviour of biomaterials: Surface for biocompatibility, J. Mater. Sci. Mater. Med., **17**, pp. 1057-1062.
- [8] Rao B.V.A., Iqbal M.Y. and Sreehar B., (2010), Electrochemical and surface analytical studies of the self assembled monolayer of 5-methoxy-2-(octadecylthiol) benzimidazole in corrosion protection of copper, Electrochim, Acta, **55**, pp. 620-631.

- [9] Liu X.Y., Ma H.Y. and Hou M.Z., (2009), Self-assembled monolayers of stearic imidazoline on copper electrodes detected using electro chemical measurement, XPS, molecular simulation and FTIR, *Chinese Sci. Bull.*, **54**, pp. 374-381.
- [10] Liao Q.Q., Yue Z.W. and Zhou Q., (2009), Corrosion inhibition effect of self-assembled monolayers of ammonium pyrrolidine dithiocarbamate on copper, *Acta Phys. Chin. Sin.*, **25**, pp. 1655-1661.
- [11] Zhang D.Q., He X.M. and Kim G.S., (2009), Arginine self-assembled monolayers against copper corrosion and synergistic effect of iodide ion, *J. Appl. Electrochem.*, **39**, pp. 1193-1198.
- Ghareba G.S. and Omanovic S., (2010), Interaction of 12-aminododecanoic acid with a carbon steel surface: Towards the development of 'green' corrosion inhibitors, *Corrosion Sci.*, **52**, pp. 2104-2113.
- [12] Sahoo R.R. and Biswas S.K., (2009), Frictional response of fatty acids on steel, *J. Colloid Interf. Sci.*, **333**, pp. 707-718.
- [13] Raman R. and Gawalt E.S., (2007), Selfassembled monolayers of alkanolic acid on the native oxide surface of SS316L by solution deposition, *Langmuir*, **23**, pp. 2284-2288.
- [14] Li D.G., Chen S.H. and Zhao S.Y., (2006), The corrosion Inhibition of the self-assembled Au and Ag nanoparticles films on the surface of copper, *Colloid. Surface. A*, **273**, pp. 16-23.
- [15] Cristiani P., Perboni G. and Debenedetti A., (2008), Effect of chlorination on the corrosion of Cu|Ni 70|30 condenser tubing, *Electrochim. Acta.*, **54**, pp. 100-107.
- [16] Cristiani P., (2005), Solutions fouling in power station condensers, *Appl. Therm. Eng.*, **25**, pp. 2630-2640.